In-flight performances of grazing incidence X-ray optics on board the X-ray astronomy satellite BeppoSAX

G. Conti, L. Chiappetti, S. Molendi
CNR - Istituto Fisica Cosmica - Via E. Bassini 15 - 20133 Milano - Italy
B. Sacco, G. Cusumano, G. La Rosa, M.C. Maccarone, T. Mineo
CNR - Istituto Fisica Cosmica - Via U. La Malfa 153 - 90146 Palermo - Italy
G. Boella
Dipartimento di Fisca - Universita' di Milano - Via Celoria 16 - 20133 Milano - Italy
O. Citterio
Osservatorio Astronomico di Brera / Merate - Via E. Bianchi 46 - 22055 Merate - Italy

ABSTRACT

The scientific instrumentation on board the X-ray Astronomy Satellite BeppoSAX, launched at the end of April 1996, includes four identical Mirror Units, each composed of 30 nested grazing incidence mirrors. The focal plane detectors are 3 identical position sensitive Medium Energy Gas Scintillation Proportional Counters, operating in the energy range 1.3-10 keV and 1 Low Energy Gas Scintillation Proportional Counter in the range 0.1-10 keV. During the Science Verification Phase (July-November 96) a selected number of X-ray targets has been observed in order to have an in-flight calibration of the instrument. This paper describes some results with particular emphasis to the on axis and off axis behaviour of the optical systems.
Keywords: X-ray optics, X-ray spectrometers, X-ray imaging, X-ray astronomical payloads.

1. INTRODUCTION

1.1 Scientific objectives

The X-ray astronomy satellite SAX [1], named BeppoSAX after launch, in honour of Giuseppe (Beppo) Occhialini, is a major program of the Italian Space Agency (ASI) with the participation of the Netherlands Agency for Aerospace Programs (NIVR). Prime industrial contractors are Alenia Spazio for the space segment and Nuova Telespazio for the ground segment.

BeppoSAX is the first X-ray mission (and, of the coming near-future satellites, the only one) that has the capability of observing sources over more than three decades of energy - from 0.1 to 300 keV - with a relatively large area, a good energy resolution, associated with imaging capabilities (resolution of about 1') in the range of 0.1-10 keV. Given the instrument capabilities over the wide energy range, BeppoSAX can provide a significant contribution in several areas of X-ray astronomy such as:

- Compact galactic sources: shape and variability of the continuum; narrow spectral features (iron line, cyclotron lines) as a function of the orbital and rotational phases; ultra-soft sources; discovery and study of X-ray transients.
- Active Galactic Nuclei: spectral shape and dynamics of the variable continuum and of the narrow and broad components from 0.1 to 200 keV in bright objects (soft excess, warm and cold absorption and related O and Fe edges, iron line and high energy bump, high energy cut-off); spectral shape of objects down to 1/20 of 3C273 up to 100-200 keV; spectra of high redshift objects up to 10 keV.
- Clusters of galaxies: spatially resolved spectra of nearby objects and the study of temperature gradients and cooling flows; chemical composition and temperature distribution as a function of redshift.
- Supernova remnants: spatially resolved spectra of extended remnants; spectra of Magellanic Cloud remnants.
- Normal galaxies: spectra from 0.1 to 10 keV of the extended emission.

SPIE Vol. 3113 • 0277-786X/97/$10.00

- Stars: multi-temperature spectra of stellar coronae from 0.1 to 10 keV.
- Gamma-ray bursts: temporal profile with 1 msec resolution from 60 to 600 keV. X-ray counterparts of a subset with position accuracy < 5'.

1.2 The payload

The BeppoSAX scientific payload consists of a set of 4 coaligned Narrow Field Instruments (NFI), namely:

1. Medium Energy Concentrator Spectrometer (MECS) [2] in the range 1.3-10 keV
2. Low Energy Concentrator Spectrometer (LECS) [3] in the range 0.1-10 keV
3. High Pressure Gas Scintillation Proportional Counter (HPGSPC) [4] in the range 3-120 keV
4. Phoswich Detector System (PDS) [5] in the range 15-300 keV

- and of two coded mask proportional counters, Wide Field Cameras (WFC), [6] in the range 2-30 keV, pointing in opposite directions and perpendicular to the NFI, to monitor large regions of the sky with a resolution of 5', to study long term variability of sources down to 1 mCrab and to detect X-ray transient phenomena.
- The anticoincidence scintillator shields of the PDS is used as an independent detector the for gamma-ray burst in the range 60-600 keV.

MECS and LECS include grazing incidence X-ray optics. The MECS consists of three identical instruments, each composed by a Mirror Unit (MU) with a Xenon filled position sensitive Gas Scintillation Proportional Counter (GSPC) in the focal plane, at the two ends of carbon fibre tubes; a fourth identical MU is used for the LECS. The MUs are composed of 30 nested coaxial and confocal mirrors with double cone geometry to approximate the Wolter I configuration. The diameters of the mirrors range from 162 to 68 mm, the total length is 300 mm, with thickness from 0.4 to 0.2 mm; the MU focal length is 1850 mm. A replica technique by nickel electroforming from super-polished mandrels was used for making the mirrors. Two front end stainless steel spiders with eight arms, in which precise grooves are machined, support and align the nested mirrors. The results of the acceptance tests of the four Flight Model MUs were published in a previous paper [7]; therein the references to the papers that describe the mirror fabrication technology can be found.

The GSPCs of the MECS [8] have an energy resolution of ~ 8.0 % at 5.9 keV and a position resolution of ~ 0.5 mm (corresponding to ~ 1 arcmin) at the same energy. The gas cell is composed by a cylindrical ceramic body (96 mm internal diameter) closed at the top by a 50 μm thick entrance Beryllium window with 30 mm diameter and on the bottom by an UV exit window in Suprasil quartz with 80 mm diameter and 5 mm thickness. The input window is externally supported by a Beryllium strongback structure, 0.5 mm thick, which consists of a ring (10 mm inner diameter, 1 mm width) connected to the window border by four ribs. Two Fe^{55} collimated calibration sources, with an emission rate of about 1 count per second, are located, diametrically opposed, near the edge of the Be window. Two grids inside the cell separate the absorption/drift region (20 mm depth) from the scintillation region (17.5 mm depth). The internal top surface around the Be window is metallized with 2 μm of Nickel to allow good uniformity of the electric field in the central region of the cell. The UV readout system consists of a crossed-wires anode position sensitive photomultiplier with a typical quantum efficiency of 20 % at the wavelength produced by the scintillation process (~ 170 nm). The duration of the light pulse (Burst Length, BL) is used to discriminate genuine X-rays against induced background or events absorbed directly in the scintillation region.

The in orbit ion shielding of the detectors is accomplished in two ways:

1. by an Au coated tungsten grid, with a transparency of 0.921, kept at +28 Volts and placed just at the output of the MUs
2. by a passive window made of a thin (0.6 μm) layer of aluminised Lexan (from Luxel) for detectors 2 and 3 and of aluminised Kapton, 7.6 μm thick, for detector 1.

An extensive end-to-end ground calibration of the 3 MECS instruments was performed at the X-ray Panter Facility of Max Planck Institute in Munich and the results were published in previous papers [2,9].

1.3 Strategy and operations

BeppoSAX was launched by an Atlas G-Centaur directly into a 600 km orbit at 3.9 degrees inclination on April 30 1996 at 4:31 GMT. The satellite nearly avoids the South Atlantic Anomaly and takes full advantage of the screening effect of the Earth magnetic field in reducing the cosmic ray induced background. Furthermore the choice of this orbit minimises the

modulation of the earth magnetic cut-off and consequently the modulation of the particle induced background. This is important in order to achieve the necessary sensitivity for observations of weak sources by the high energy experiments, particularly for the PDS.

The satellite achieves one arc-minute pointing stability with the same post facto attitude reconstruction accuracy. The main attitude constraint derives from the need to maintain the normal to the solar arrays within 30 degrees from the sun, with occasional excursions to 45 degrees for some WFC observations. Therefore, during a single orbit, the NFI have a 60 degrees band in the sky available for observations (50% of the sky), and the WFC a slightly larger region. Observing efficiency depends on target position due to the possible eclipse by Earth (which has a diameter of about 130° at 600 km).

While the NFI are the prime instruments most of the time, the WFC are periodically used to scan the galactic plane to monitor the temporal behaviour of sources above 1 mCrab and to detect transient phenomena. Thanks to their large field of view, the WFC are operated to monitor selected objects when the NFI perform their sequence of pointed observations. The observing programs are held flexible in order to accommodate those Targets Of Opportunity (TOO) for follow-up observations with the NFI, that can be done within a few hours from the discovery, due to BeppoSAX prompt control and operation capabilities. The observations are organised on the basis of a "Core Program", devoted to systematic studies with particular regard to scientific objectives that exploit BeppoSAX characteristics, and of a "Guest Observer" program.

The satellite passes every orbit above the ground station, placed near the equator (Malindi, Kenya), with a contact duration of 10 minutes. During each orbit up to 450 Mbit of data are stored onboard and relayed to ground during station passage. The average data rate available to instruments will be about 70 kbit/s, but peak rates of up to 100 kbit/s can be retained. The Operational Control Centre (OCC), located in Rome at Nuova Telespazio, is connected to the ground station by a relay satellite. The Scientific Data Centre is located in the same place of the OCC, to optimise the interaction between the scientific and operational components.

The satellite commissioning phase ended on July 12, 1996 and the Science Verification Phase (SVP) on December 4, 1996 although most of the observation were completed within 22 September and the Core Program had started as early as August. The goal of the SVP was to verify the expected scientific capabilities of the mission and to perform an in-flight calibration of the instruments. To this aim a series of objects with well known properties have been selected and observed.

This paper presents the in flight performances of the MECS, compared with the ground calibrations.

2. IN-FLIGHT PERFORMANCES OF MECS MIRROR UNITS

2.1 On-axis Point Spread Function

The three MECS instruments onboard the BeppoSAX satellite exhibit very similar behaviour. We report here as reference the results of the analysis for the MECS unit 3.

The Point Spread Function (PSF) of the MECS is the convolution of the mirror unit PSF [7] and the detector PSF. We have used the "first light" on-axis pointing on Cyg X-1 to measure the PSF and to compare it with the analytical on-axis PSF model that has been developed from the ground calibrations [2]. Fig. 1 shows the differential PSF in six selected energy bands, chosen to match the energies used during the ground calibrations. The solid curve is the Gaussian + generalized Lorentzian model [2] derived from the calibrations, normalized to the peak intensity. The glitch on the data at about 600 arcsec for the lower energies is due to the absorption of the window strongback. The excellent statistics allows to sample the wings of the PSF up to the outer edges of the detector field of view. The good agreement between the model and the measured points is an indication that the MUs have not suffered geometrical distortions during the launch phase.

The detailed analysis of the off-axis PSF is currently under way but we have already a clear indication that, for off-axis angles < 10 arcmin (that corresponds to the region of the detector inside the window strongback), the departure of the PSF shape from radial symmetry is very small, thus allowing us to apply the same radial description of the on-axis PSF; this is qualitatively demonstrated by Fig. 2, which shows a composite image combining 6 successive pointing on Cyg X-1: on-axis and, in order, at 3.6, 6.4, 13.5, 18.8 and 24.3 arcmin off-axis.

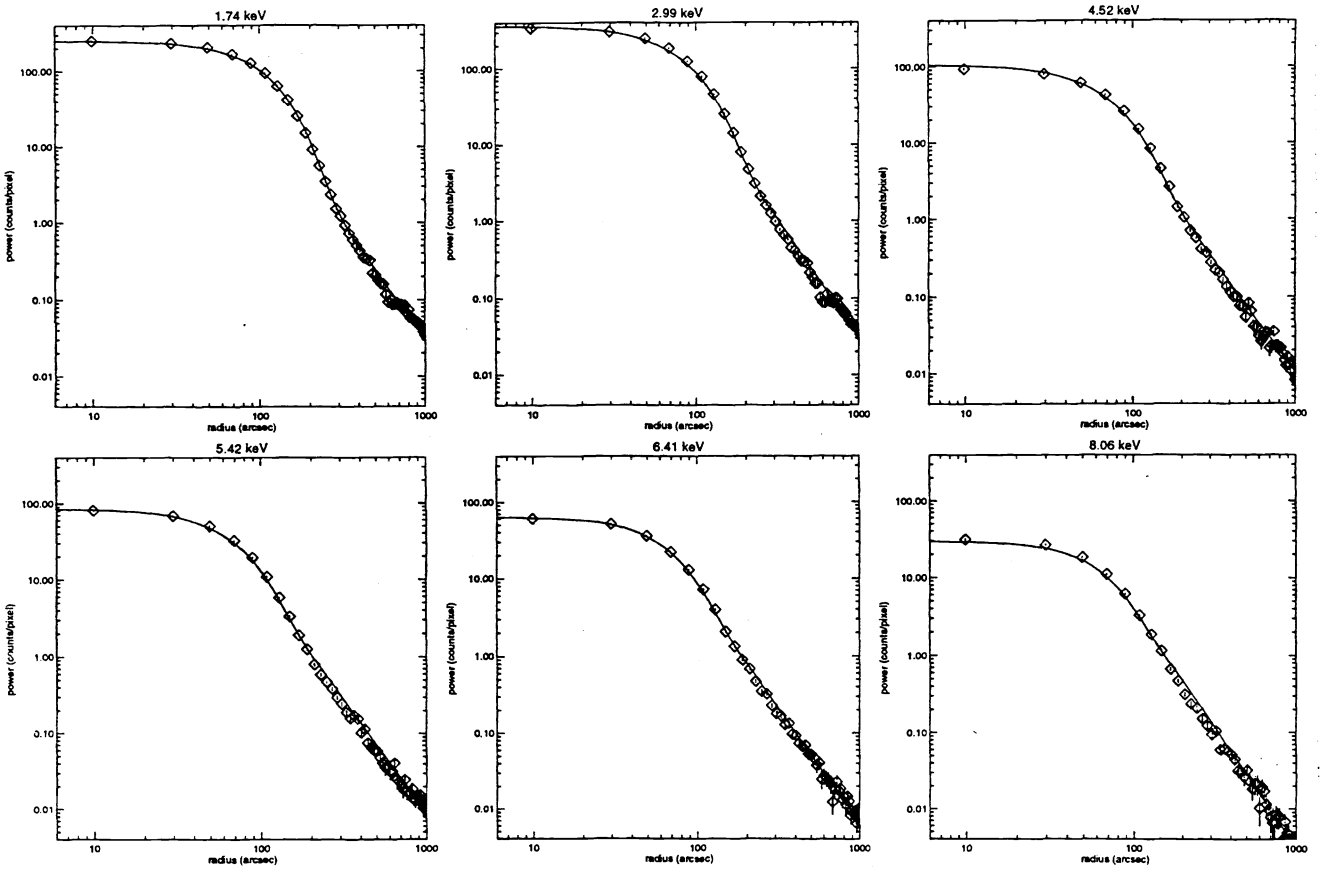

Fig.1 - MECS unit 3: differential PSF in six energy bands. The solid line is the model derived from ground calibrations.

2.2 Mirror efficiency

The effective area of the mirror units has been measured during ground calibrations at several energies [2]. The interpolation and extrapolation of these values over the MECS range are obtained reducing the mirrors total geometric area by the square of the gold reflectivity, computed using the Henke coefficients [10]. The agreement with the experimental results has been reached by multiplying the theoretical values with a second order polynomial of energy. The best polynomial parameters are obtained by fitting experimental data. A small discrepancy was present only for the MECS unit 3 below 2 keV (see dashed line in Fig. 3). Moreover, another correcting factor is applied to take into account the loss of efficiency for the Panter beam divergence. This factor is defined as the ratio of the effective area for a source at infinite distance computed with a ray-tracing code, and the Panter observed values.

The on-ground calibration results have been tested in-flight by fitting the observed spectrum of the Crab nebula with the canonical power law with interstellar absorption. Data are well modelled over the whole band except at the gold absorption edge where a line-type residual is apparent. The origin of this feature is either due to a not perfect modelling of the gold reflectivity at the edges, or to the difficulty to know the energy-channel relation with the precision required by the large gradient of the effective area. In order to reduce the residuals in the Crab fit, an "ad-hoc" correction has been introduced in the on-axis effective area of each unit adding a gaussian whose mean energy, amplitude and width have been determined fitting the Crab spectrum with an absorbed power law plus a line. Furthermore, for the MECS unit 3, it was also necessary to recompute the parameters of the second order polynomial to correct the discrepancy at low energy. Fig. 3 shows the final on-axis optics effective area (continuous line) superimposed to the ground calibration (dashed line).

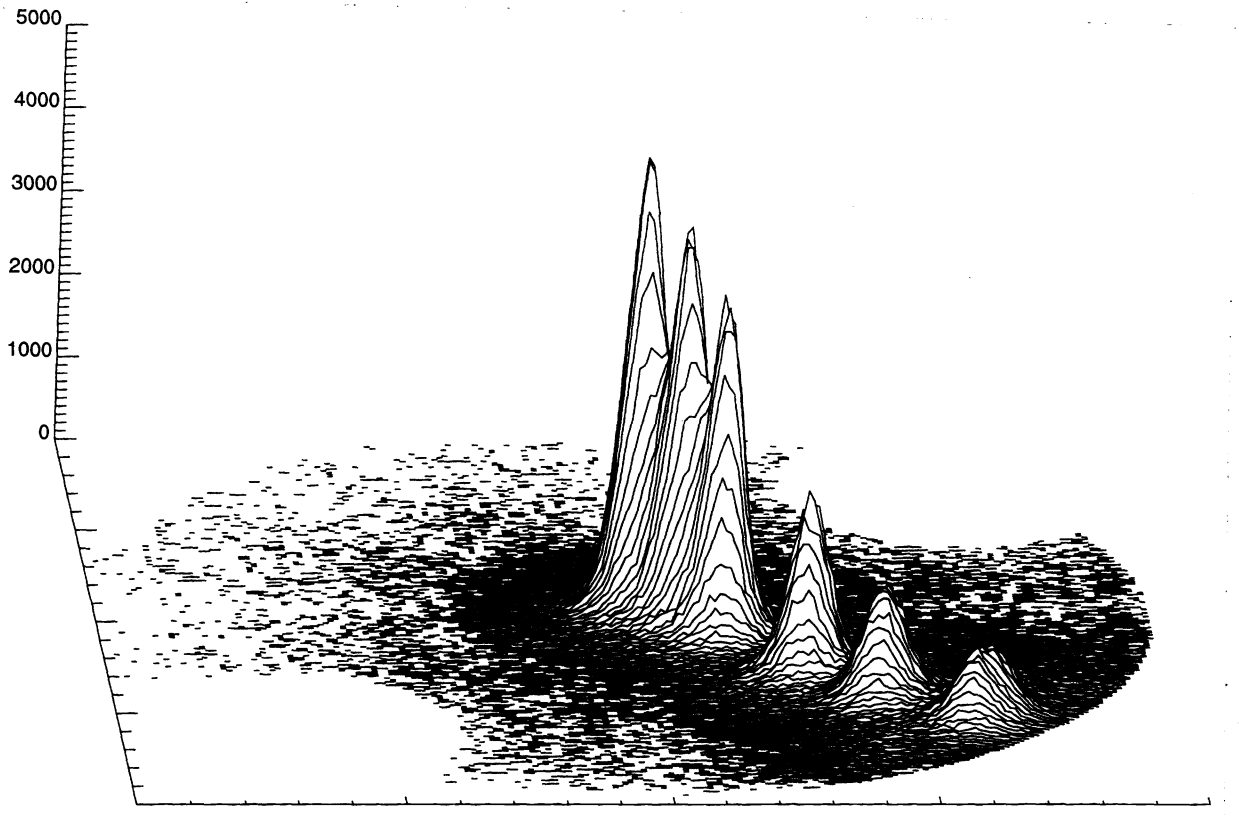

Fig. 2 - Composite image combining six observation of Cyg X-1 with MECS unit 3 at different off-axis angles (see text). Intensities have been normalized to the same exposure time (7355 sec).

The on-axis flux measured on Crab, which is within few percent of the expected one, gives us also the information that the optics of the MUs have not suffered from surface contamination during the integration and the alignment on the satellite and during the launch phase. The final residuals of the Crab spectrum fit are within 3% for each MECS unit. As example, the ratio of the data to the model is reported in Fig. 4 for MECS unit 3. The values of the fit parameters are: 2.09 ± 0.02 for the photon spectral index, $2.92 \cdot 10^{21}$ cm^{-2} for the absorbing column and 8.43 ± 0.03 photons/cm^2/sec/keV for the normalisation at 1 keV.

The decrease of effective area as a function of the off-axis angle (vignetting factor) has been measured during ground calibrations using a discrete set of energy lines. The data analysis showed that the vignetting factor is function of energy: as example, for Al (1.49 keV) and Cu (8.04 keV) lines, the measured vignetting factor is reported in Fig. 5 (dashed lines). During the SVP in-flight calibration, five pointing of Crab at different off-axis angles (1.5, 5.4, 13.2, 18.7, 30 and 45 arcmin; see also Fig. 6) have been performed to confirm the on-ground vignetting results and to have information about the stray X-ray contamination (see next section). Fig. 5 shows the results for the MECS unit 3, where the source countrate has been normalised to the on-axis value. Data have been fitted with the relation $1/(1+A \cdot r^B)$ where the best values for A and B are respectively 0.013867 and 1.662397, and r is expressed in arcmin. The in-flight result is in good agreement with the calibrations: in fact the curve is representative of an intermediate energy, since the spectrum is accumulated in the energy range 1.5 - 10 keV.

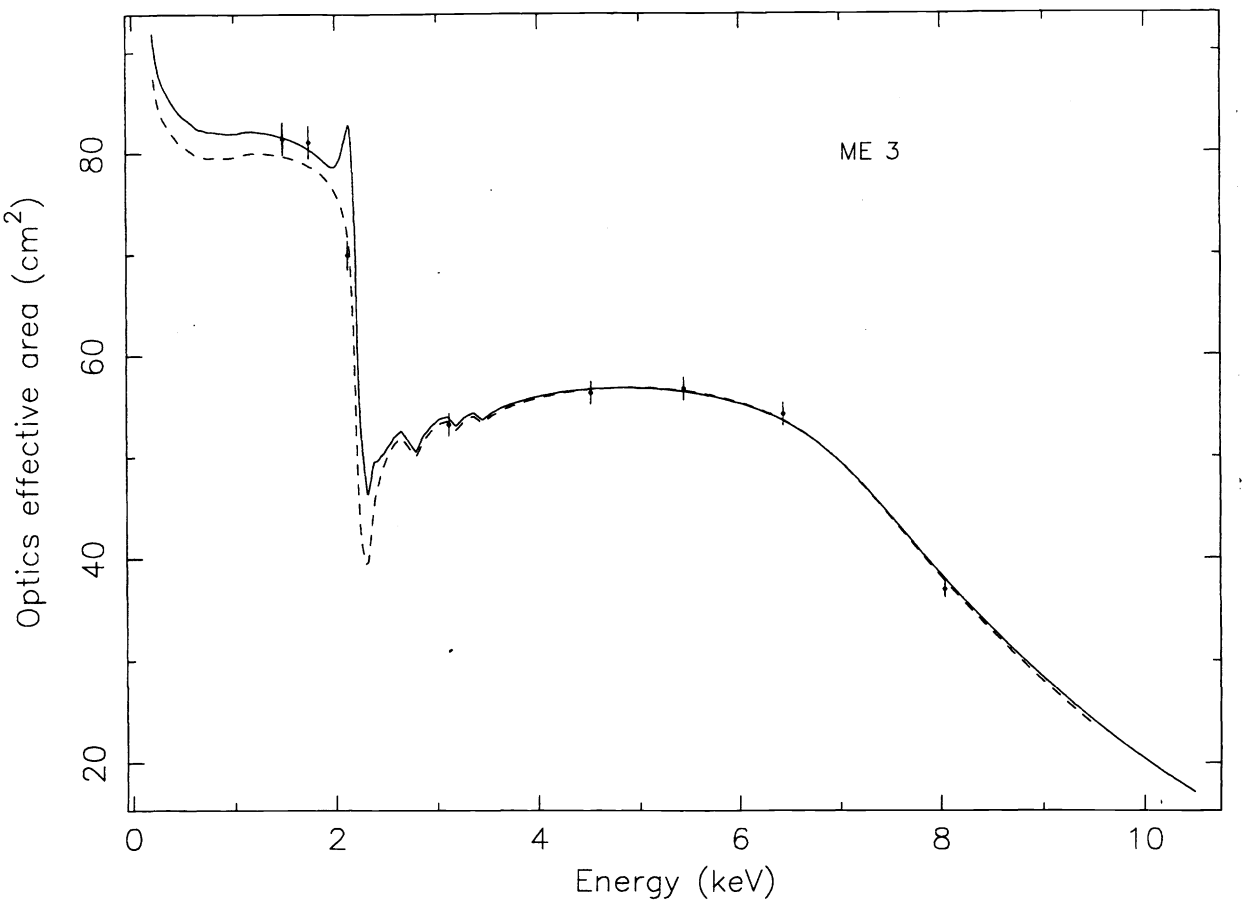

Fig. 3 - Final on-axis optics effective area vs. energy for the MECS unit 3 (continuous line). The markers refer to the ground calibration measurements and dashed line represents the relevant preliminary effective area derivation [2].

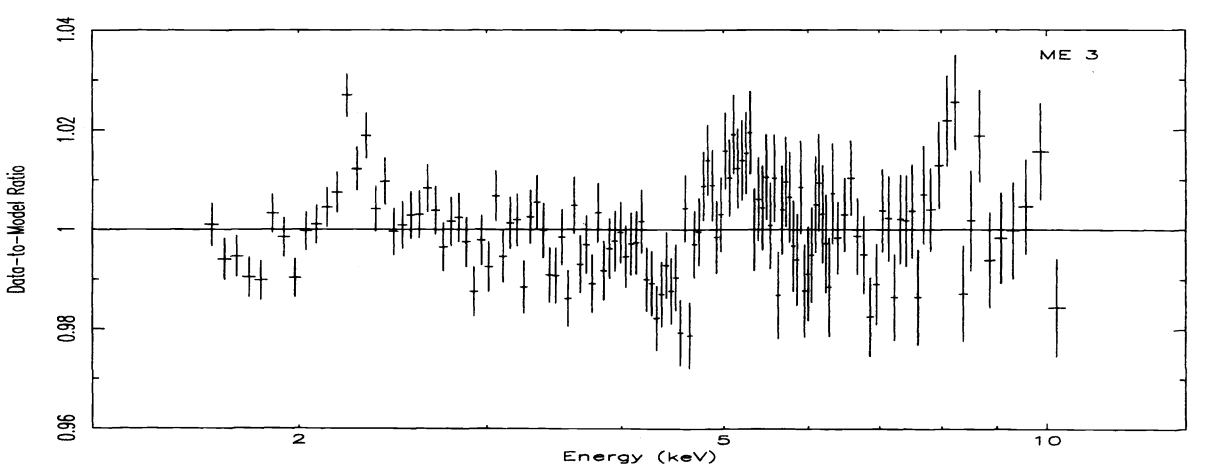

Fig. 4 - Residuals of a fit to the Crab spectrum for the MECS unit 3, expressed as the ratio of the data to the model

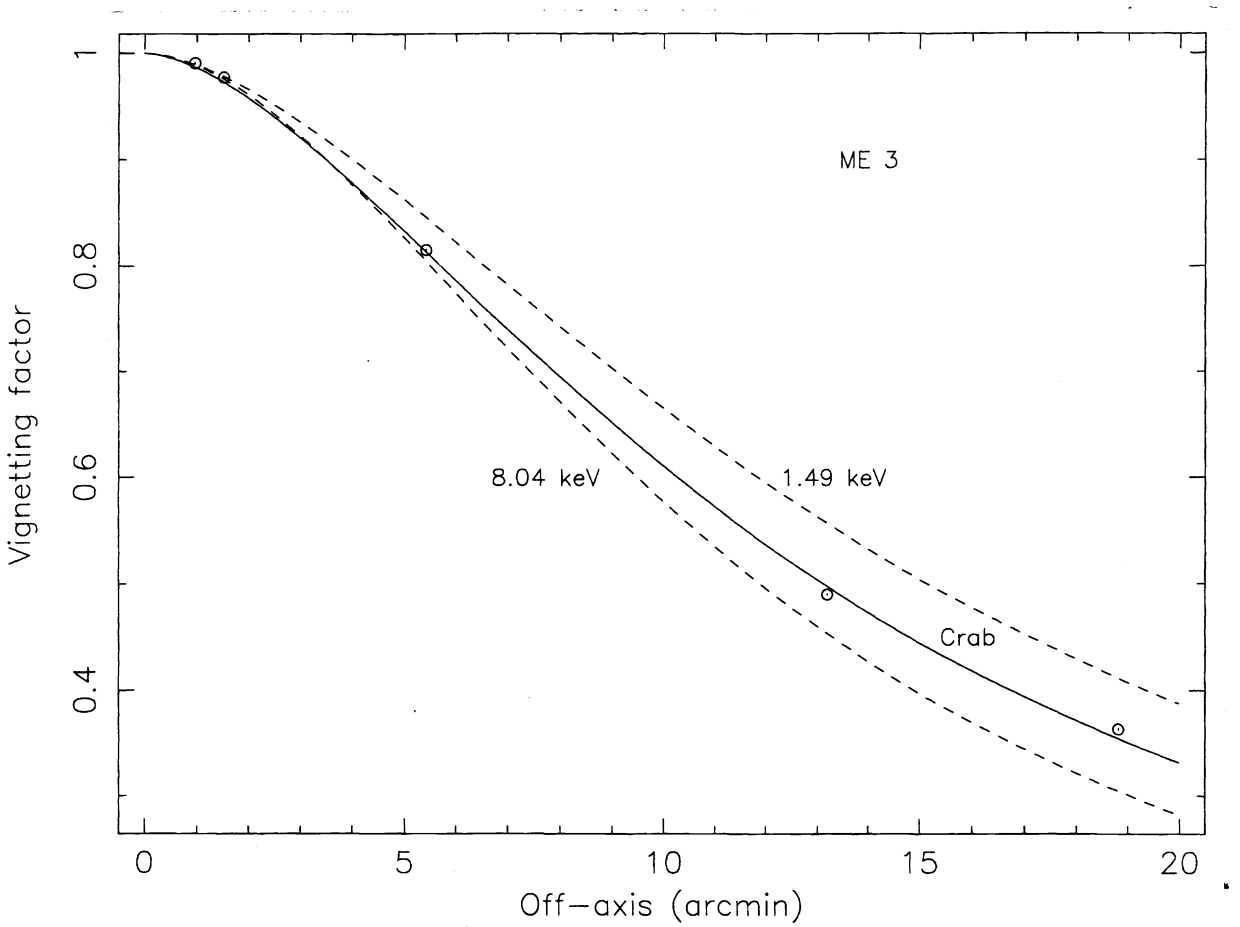

Fig. 5 - Vignetting factor vs. off-axis angle for the MECS unit 3. Dashed lines refer to the ground calibrations; experimental points and the relevant fitted curve refer to the in-flight SVP calibration on the Crab nebula.

Fig. 6 show the contour maps of MECS unit 3 images for the Crab off-axis observations. We recall that the MECS field of view is 28 arcmin radius. Data have been normalized to the same exposure (8011 sec) and contour levels are logaritmically spaced, with 3 levels per decade. The levels for exact decades are indicated with thicker lines. In cases (e) and (f) the target is outside the field of view (see also Fig. 7 and Fig. 8).

2.3 Stray X-ray contamination

The presence of a strong X-ray source in the neighbourhood of the field of view contaminates the internal field of the MECS instruments. The contamination is due to X-rays which do not follow the normal double-reflection way, but have either one single reflection or no reflection at all. We distinguish three cases:

1. primary single reflection photons: X-ray photons which are reflected by the primary optics (entrance half cones) but not intercepted by the secondary optics (exit half cones)
2. secondary single reflection photons: X-ray photons which are intercepted only by the secondary optics
3. direct photons: X-ray photons, crossing the optics system and arriving on the detector focal plane, without any interaction with the double-cone mirrors system.

The total countrate, shape, relative ratio, and mutual distance of the three components depend from the off-axis distance of the source; the intensity is also proportional to the source strength.

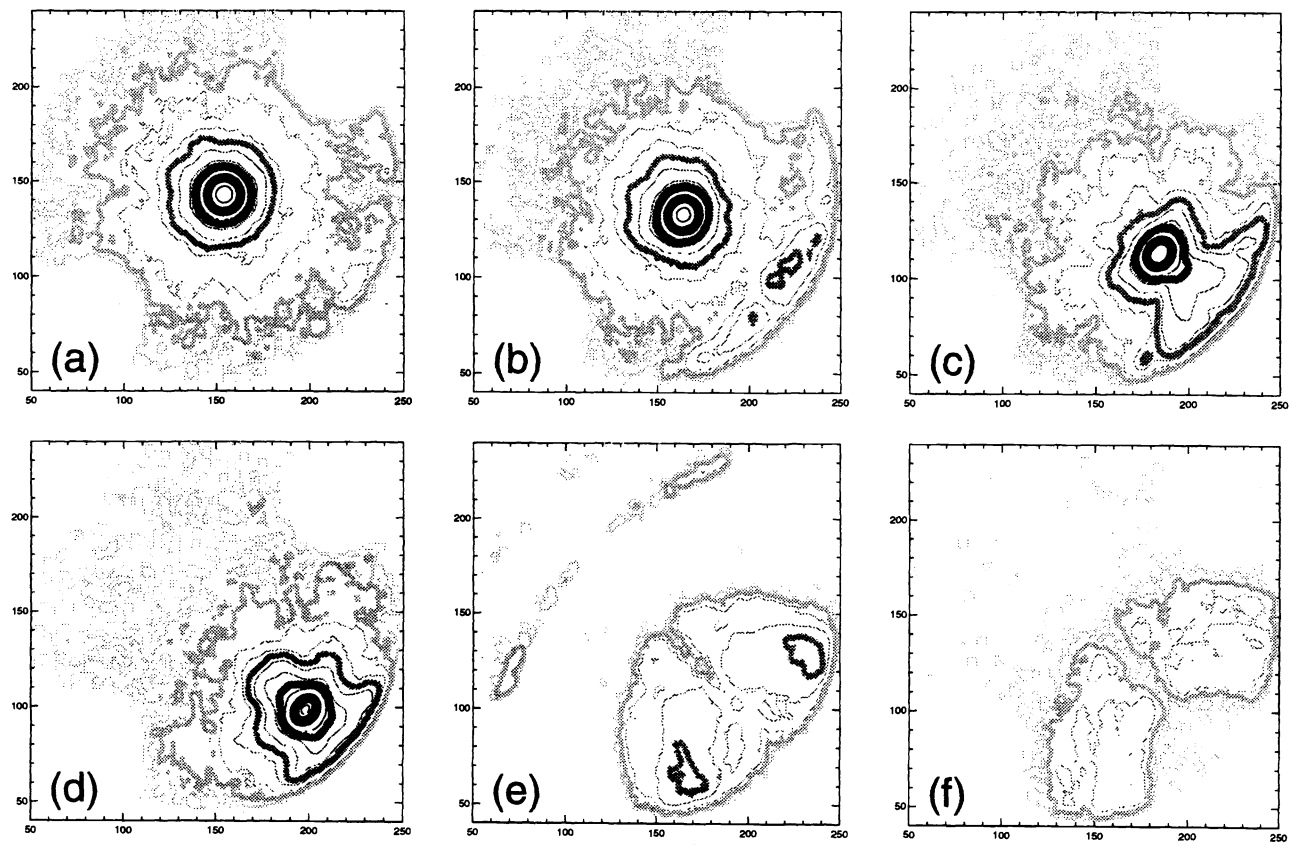

Fig. 6 - MECS unit 3. Contour maps of six observations of the Crab nebula at different off-axis angles: (a) 1.5 arcmin; (b) 5.4 arcmin; (c) 13.2 arcmin; (d) 18.7 arcmin; (e) 30 arcmin; (f) 45 arcmin (see text).

Fig. 7 and Fig. 8 show, in a different representation, the data of Fig. 6(e) and Fig. 6(f). The fraction of the Crab signal in the field of view is 0.041 ± 0.001 when Crab is at 30 arcmin (see Fig. 7), and 0.015 ± 0.001 in the case of 45 arcmin off-axis (see Fig. 8). The enhancement on the right down side of Fig. 7 is due to single reflection photons, while the arc shaped images on the left upper side are due to the direct photons. In the case of Fig. 8 (45 arcmin off-axis), the direct photons are no more visible. In both the figures, the lack of photons along the diagonal is due to the shadow of the spider system.

ACKNOWLEDGEMENTS

We would like to thank R.C.Butler, BeppoSAX payload manager and flight director, for his tireless effort in supporting the BeppoSAX mission. Thanks are due to the teams of Alenia Spazio, Laben and Nuova Telespazio for their professional job on the satellite, on the payload and on the ground segment. All the activities of the Scientific Institutes have been financially supported by the Italian Space Agency in the framework of the SAX mission.

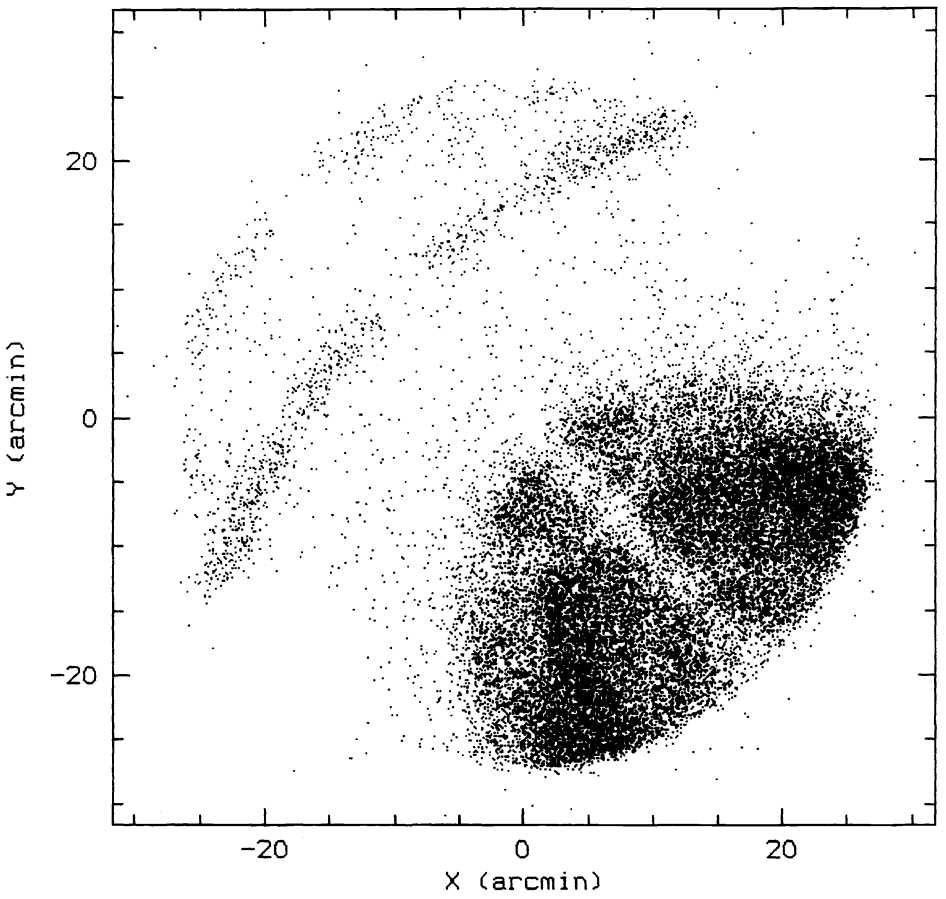

Fig. 7 - Pointing 30 arcmin far from the Crab source. Field of view of MECS unit 3

REFERENCES

1 G. Boella, R.C. Butler, G.C. Perola, L. Piro, L. Scarsi and J. Bleeker, "BeppoSAX, the wide band mission for X-Ray Astronomy", *A&A Suppl.* 122, 299, April (II) 1997.

2 G. Boella, L. Chiappetti, G. Conti, G. Cusumano, S. Del Sordo, G. La Rosa, M.C. Maccarone, T. Mineo, S. Molendi, S. Re, B. Sacco and M. Tripiciano, "The medium-energy concentrator spectrometer on board the BeppoSAX X-ray astronomy satellite", *A&A Suppl.* 122, 327, April (II) 1997.

3 A. N. Parmar, D.D.E. Martin, M. Bavdaz, F. Favata, E. Kuulkers, G. Vacanti, U. Lammers, A. Peacock and B.G. Taylor, "The low-energy concentrator spectrometer on board the SAX X-ray astronomy satellite", *A&A Suppl.* 122, 309, April (II) 1997.

4 G. Manzo, S. Giarrusso, A. Santangelo, F. Ciralli, G. Fazio, S. Piraino and A. Segreto, "The High Pressure Gas Scintillation Proportional Counter on board the BeppoSAX X-ray Astronomy Satellite", *A&A Suppl.* 122, 341, April (II) 1997.

5 F. Frontera, E. Costa, D. Dal Fiume, M. Feroci, L. Nicastro, M. Orlandini, E. Palazzi and G. Zavattini, "The high energy instrument PDS on board the BeppoSAX X-ray astronomy satellite", *A&A Suppl.* 122, 357, April (II) 1997.

6 R. Jaeger, W.A. Mels, A.C. Brinkmann, M.Y. Galama, H. Goulooze, J. Heise, P. Lowes, J.M. Muller, A. Naber, A. Rook, R. Schuurhof, J.J. Schuurmans and G. Wiersma, "The Wide Field Camera on board the BeppoSAX X-ray Astronomy Satellite", *A&A* in press.

7 G. Conti, E. Mattaini, E. Santambrogio, B. Sacco, G. Cusumano, O. Citterio, H. Brauninger, and W. Burkert, "X-ray characteristics of SAX flight mirror units", *Proc. SPIE* 2279, 101, 1994.

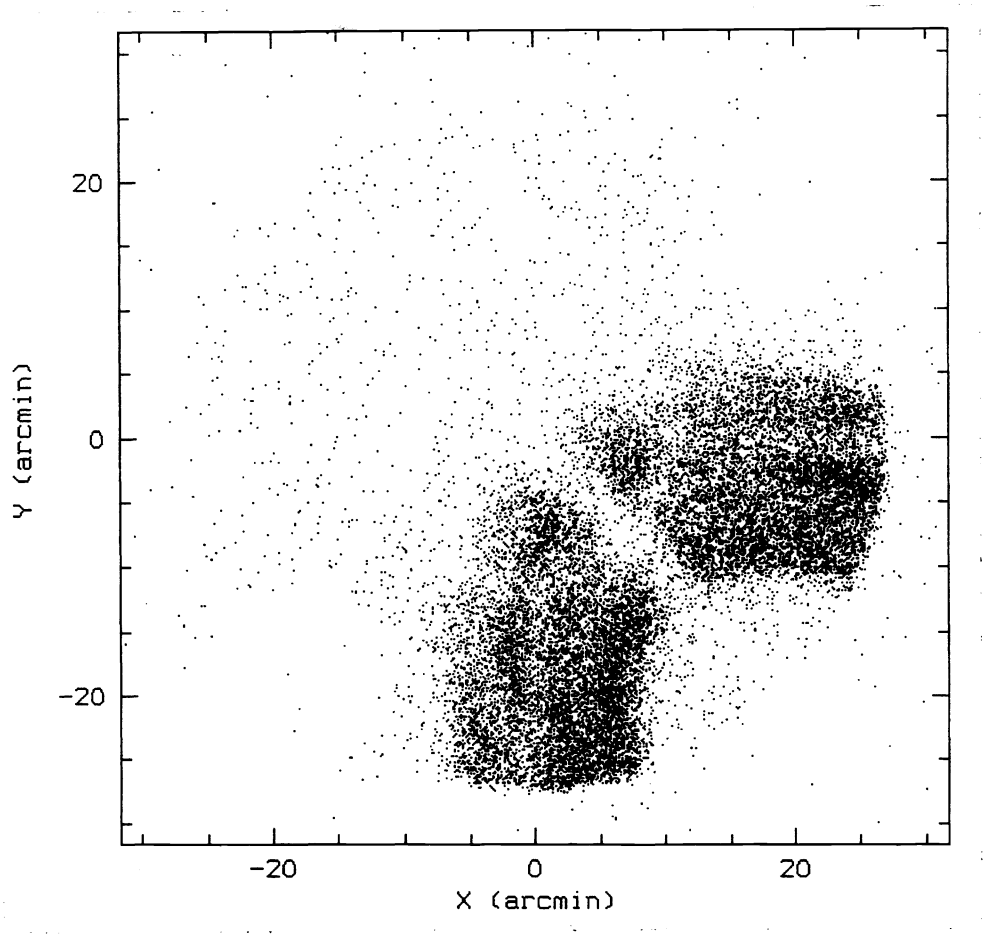

Fig. 8 - Pointing 45 arcmin far from the Crab source. Field of view of MECS unit 3

8 A. Bonura, S. Giarrusso, L. Lombardo, G. Manzo, S. Re, G. La Rosa, F. Celi, R. Di Raffaele, G. Conti, H. Brauninger, and W. Burkert, "Performance characteristics of the Scientific Model of the Medium Energy Concentrator Spectrometer on board the X-ray Astronomy Satellite SAX", *Proc. SPIE* 1743, 510 ,1992.

9 G. Boella, L. Chiappetti, G. Conti, S. Molendi, G. Cusumano, S. Del Sordo, G. La Rosa, M.C. Maccarone, S. Re, B. Sacco, M. Tripiciano, H. Brauninger and W. Burkert, "Medium Energy Concentrator Spectrometer on board the X-ray Astronomy Satellite SAX. Preliminary results of ground X-ray calibrations", *Proc. SPIE* 2517, 223, 1995.

10 B.L. Henke., E.M. Gullikson, J.C. Davis, *Atomic Data and Nuclear Data Tables* 54-2, 1, 1993.

Further information:
BeppoSAX WEB site: http://www.sdc.asi.it
MECS home page: http://sax.ifctr.mi.cnr.it/Sax/Mecs
G. Conti Email conti@ifctr.mi.cnr.it